Reverse time migration of internal multiples

Yike Liu and Hao Hu, Institute of Geology and Geophysics Chinese Academy of Sciences; Xiao-Bi Xie, University of California at Santa Cruz; Yingcai Zheng, University of Houston*

SUMMARY

Internal multiple reflections have different propagation paths compared with primary reflections and surface-related multiples, thus can complement illuminations where other waves are unavailable. We propose a novel approach to image structures with internal multiples. With this method, internal multiples are separated and used as data for reverse time migration. Instead of applying image condition directly to the source and receiver waves, we decompose both source and receiver waves extrapolated into up- and down-going waves. Then apply the image condition to up-going source and receiver waves to form an up-up image, and apply to down-going source and receiver waves to form a down-down image. The image from the true reflector and the artifact show different features in the down-down and up-up images. We use a similarity analysis to compare the up-up and down-down images, and separate true images from artifacts. Numerical examples with simple velocity models are used to demonstrate how to construct up-up and down-down image conditions and eliminate migration artifacts. Finally, we test the 2D SMAART JV model with salt structures for migration using internal multiples.

INTRODUCTION

Internal multiples are waves reflected more than once at interfaces before reach to the surface receivers. Internal multiples are usually generated below coal seams, salt domes, basalt and igneous rocks with high velocity contrast, and behave differently compared to primary reflections and surface-related multiples. They often travel longer distances, cover larger areas than primary reflections, and can provide additional illumination to shadow zones of primary reflections. Although primary reflections provide important information for seismic imaging, surface related and internal multiples are also valuable. Even with these advantages, to extract useful information from multiples is not easy. Compared with surface related multiple imaging, few attempts have been made for migration of internal multiples. Jin et al. (2006) used one return propagator to extrapolate both down- and up-going duplex waves to image steep structures. Target-orientated interferometry is another approach of using internal multiples for imaging (Vasconcelos et al., 2007; Jiang et al., 2007). Malcolm et al. (2008) developed an inverse generalized Bremmer coupling series to image triply scattered waves in one-way wave equation based migration. To utilize the multiply scattered data, Fleury (2013) proposed a nonlinear reverse time migration. Zuberi and Alkhalifah (2014) developed a generalized internal multiple procedure to realize migration of internal mutliples. Recently, a promising approach based on the Marchenko equation was proposed for imaging internal multiples (e.g., Behura, et al., 2012; Broggini, et al., 2013; Neut et al., 2013; Thorbecke, et al., 2013; Wapenaar, et al., 2014; Slobe, et al., 2014; Singh et al., 2014).

In this paper, we present a reverse time migration (RTM) method capable of handling internal multiples. The method first extracts internal multiples, followed by extrapolating multiples backward in time to subsurface. Both extrapolated source and receiver wavefields are decomposed into up- and down-going waves. A crosscorrelation imaging condition is applied to these decomposed waves, and generates images from waves propagating in different directions. By comparing images from up-going waves with images from down-going waves, the artifacts can be recognized and attenuated. In the rest part of this paper, we first review the internal multiple prediction method, and investigate how to migrate internal multiples to form correct images. Finally, we discuss the efficacy of this method and demonstrate its applications using synthetic examples.

THEORY AND METHOD

Predicting and extracting internal multiples

Internal multiples bear different kinematic and dynamic characteristics compared to primary reflections and surface-related multiples. Verschuur et al. (1992) and Berkhout (1997) provided theoretical insights for wave-equation based surface-related multiple elimination (SRME), which has been widely used in the industry since then. Jakubowicz (1998) extended this technique to attenuate internal multiples. Based on inverse scattering series (ISS), Weglein et al. (1997, 2013) developed another method to predict internal multiples. The advantage of the ISS-based methods is that they only require background velocity information and are fully data-driven. Internal multiples from all origins, including their arrival times and approximate amplitudes can be predicted without knowing detailed subsurface structure. Both methods are utilized in this paper.

Image conditions for migrated internal multiples

We modify the conventional image condition by separating it into two groups, those generated by a pair of down-going waves are named as down-down (DD) images, and those generated by a pair of up-going waves are named as up-up (UU) images. As shown in Figure 1, applying DD and UU image conditions can generate 4 groups of images

DOI http://dx.doi.org/10.1190/segam2015-5760515.1

$$
\begin{aligned}
I(\boldsymbol{r}) &= \sum_{t=0}^{T} S(\boldsymbol{r},t)R(\boldsymbol{r},T-t) \\
&= \sum_{t=0}^{T}\left[S_U(\boldsymbol{r},t)+S_D(\boldsymbol{r},t)\right]\left[R_U(\boldsymbol{r},T-t)+R_D(\boldsymbol{r},T-t)\right] \\
&= I_{UU}(\boldsymbol{r})+I_{DD}(\boldsymbol{r})+I_{UD}(\boldsymbol{r})+I_{DU}(\boldsymbol{r}),
\end{aligned} \tag{1}
$$

where *S* and *R* are for source and receiver waves, subscripts *U* and *D* are for up- and down-going directions,

$$I_{UU}(\boldsymbol{r}) = \sum_{t=0}^{T} S_U(\boldsymbol{r},t)R_U(\boldsymbol{r},T-t)\,, \tag{2}$$

$$I_{DD}(\boldsymbol{r}) = \sum_{t=0}^{T} S_D(\boldsymbol{r},t)R_D(\boldsymbol{r},T-t)\,, \tag{3}$$

are UU and DD images. The $I_{UD}(\boldsymbol{r})$ and $I_{DU}(\boldsymbol{r})$ are mostly cross talks and will be dropped.

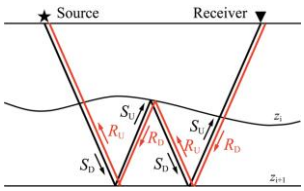

Figure 1. Cartoon showing the up- and down-going sections of source and receiver waves. The black path indicates the forward propagated wave from a source to a receiver and the red path indicates the back propagated wave from a receiver to a source. The arrows indicate the related up- and down-going source and receiver waves.

Decomposing internal multiples into up- and down-going waves

To decompose the source wavefield into up- and down-going waves, we use the 2D Fourier transform to convert the wavefield from space-time domain (x,z,t) to frequency-wavenumber domain (x,k_z,ω), followed by separating it in the *f-k* domain (Liu, et al., 2011)

$$S_D(\omega,x,k_z) = \begin{cases} S(\omega,x,k_z), & \text{if } k_z \geq 0 \\ 0, & \text{if } k_z < 0 \end{cases}, \tag{4}$$

$$S_U(\omega,x,k_z) = \begin{cases} 0, & \text{if } k_z \geq 0 \\ S(\omega,x,k_z), & \text{if } k_z < 0 \end{cases}, \tag{5}$$

where $S_{U,D}(\omega,x,k_z)$ is the transform of $S_{U,D}(\boldsymbol{r},t)$, k_z is the vertical wavenumber, ω is the angular frequency. Finally, we inverse Fourier transform $S_{U,D}(\omega,x,k_z)$ and $R_{U,D}(\omega,x,k_z)$ back to the space-time domain to obtain the required up- and down-going waves in equations 2 and 3. Similarly, we can obtain space-time domain up- and down-going wavefields for the receiver wave.

Image and artifacts generated by internal multiples

Unlike the one-way wave equation migration or Kirchhoff migration, the RTM uses full wave propagator to extrapolate the source and receiver waves. In a realistic velocity model with interfaces, the full wave propagator can generate additional reflections which form artifacts. We use Figure 2 to illustrate how to image multiples and eliminate artifacts. Shown in this figure are (z,t) domain wavefields calculated in a simple 3-layer model (refer to the model in Figure 3a). The short horizontal bars indicate the depths of two interfaces, and the velocities from top to bottom are 1500 m/s, 3000 m/s and 1000 m/s, respectively.

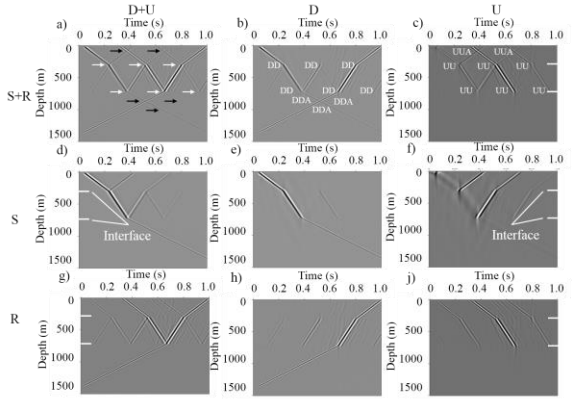

Figure 2. Migrated source and receiver wavefields in (z,t) domain. Top row: overlapped source and receiver waves, middle row: source waves, and bottom row: time-reversed receiver waves. Left column: total wavefield, middle column: decomposed down-going waves, and right column: decomposed up-going waves.

The top row is mixed source and receiver wavefileds at x=1000 m in (*z, t*) domain, the middle and bottom rows are separated source and time-reversed receiver waves. Shown in the left column are total wavefields, in the middle column are decomposed down-going waves, and in the right column are decomposed up-going waves. From the mixed source and receiver wavefields 2a, we see the source and receiver waves intersect at selected depths, where the two waves meet the zero-lag image condition and form images. However, in addition to the image from two real interfaces (indicated by white arrows), there are also artifacts (indicated by black arrows). To eliminate these artifacts, we use equations 4 and 5 to decompose the source and receiver wavefields into up- and down-going waves and use equations 2 and 3 to calculate UU and DD images. Figure 2b is for DD image, where events related to real reflectors are labeled with DD and the events related to down-going artifacts are shown as DDA. Figure 2c is for UU image, where events related to real reflectors are labeled with UU and events related to up-

DOI http://dx.doi.org/10.1190/segam2015-5760515.1

going artifacts are shown as UUA. Shown in the middle and bottom rows are decomposed source and receiver waves, which explain how these images are formed. Comparing Figures 2b and 2c, images related to real interfaces appear in both DD and UU images, while artifacts are only shown in one of these images. Hence, by comparing the DD and UU images, we can eliminate artifacts.

Artifacts attenuation based on the similarity between UU and DD images

As have been mentioned, we can attenuate artifacts by comparing the similarity between DD and UU images. To quantify this process, we use a spatial window to mosaic the DD and UU images into small areas. Within each window, we have two sequences of discretized images

$$I^i_{DD} = I_{DD}(\mathbf{r}_i), \tag{6}$$

$$I^i_{UU} = I_{UU}(\mathbf{r}_i), \tag{7}$$

where $\mathbf{r}_i$ is the location of an image pixel, $i = 1,2,3.....n$, and n is the number of pixels in the window. The similarity between the two sequences can be measured by the correlation coefficient

$$R = \frac{\sum_{i=1}^{n}\left[(I^i_{DD} - \bar{I}_{DD})(I^i_{UU} - \bar{I}_{UU})\right]}{\left[\sum_{i=1}^{n}(I^i_{DD} - \bar{I}_{DD})^2\right]^{1/2}\left[\sum_{i=1}^{n}(I^i_{UU} - \bar{I}_{UU})^2\right]^{1/2}}, \tag{8}$$

where

$$\bar{I}_{DD} = \frac{1}{n}\sum_{i=1}^{n}(I^i_{DD}) \tag{9}$$

and

$$\bar{I}_{UU} = \frac{1}{n}\sum_{i=1}^{n}(I^i_{UU}) \tag{10}$$

are mean values of images. Correlation coefficient R varies between -1 and $+1$, with $R = +1$ means the two sequences are perfectly positively correlated, while $R = -1$ means they are perfectly negatively correlated. $R = 0$ means they are totally unrelated. We set a positive threshold. If correlation coefficient of UU and DD images in the spatial window is above the threshold, this part of the image will be retained. Otherwise, it will be judged as artifact and rejected from the final image.

NUMERICAL EXAMPLES

Migration of internal multiples in a 3-layer model

We use the simple 3-layer model, shown in Figure 3a, to demonstrate our approach. The model is 2 km in horizontal and 1.5 km in depth, and is partitioned with a grid interval of 5 m in both x- and z-directions. Illustrated in Figure 3b is a common shot record, where primary reflections and surface related multiples have been taken away, thus consisting of only internal multiples. We see internal multiples up to the third order can be identified.

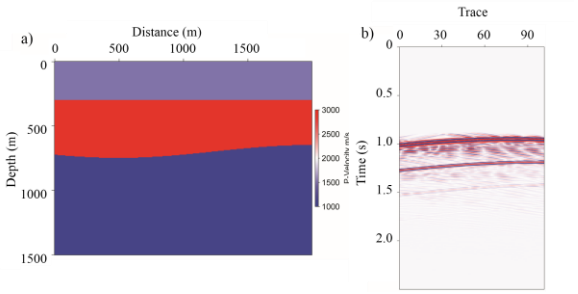

Figure 3. (a) A three-layer velocity model separated by a flat upper interface and a curved lower interface. (b) The common shot record with primary reflections eliminated, where internal multiples up to the third order can be identified.

The resulted image from internal multiples is shown in Figure 4. In Figure 4a, AF, AC AD and AE are artifacts, while TA and TB are true interfaces images. To attenuate artifacts using the process mentioned above, we decompose the extrapolated wavefields into up- and down- going waves. The artifacts have been categorized into DD and UU images (Figure 4b and 4c). The images related to the true interfaces and artifacts are similarly labeled as those in Figure 2. To attenuate artifacts, we use equation 8 to measure the similarity of DD and UU images to eliminate unwanted part. After this process, the result is shown in Figure 4d. In case artifacts intercept with an interface event, the overlapped part will be preserved, while other part will be removed.

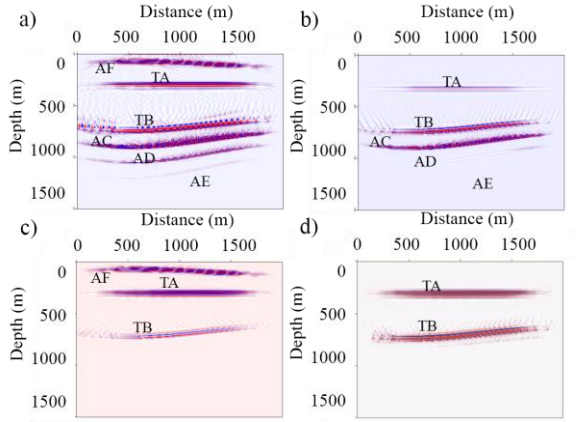

Figure 4. (a) Images from internal multiples without artifact attenuation; (b) UU image with internal multiples; (c) DD image with internal multiples; and (d) the final image from internal multiples after attenuating artifacts.

The RTM image using internal multiples in SMARRT salt data

DOI http://dx.doi.org/10.1190/segam2015-5760515.1

The 2D SMAART JV （Stoughton et al., 2001）is composed of a sequence of sedimentary layers, a number of normal and thrust faults, and several salt bodies (Figure 11). The free surface and velocity contrasts at sea bottom and top and bottom salt boundaries generate strong free surface and interbed multiples. The salt bodies generate significant multi-path and non-hyperbolic moveouts, which result in image problems for the conventional migration with primary reflections. A total of 1387 shots, with an interval of 22.86 m, are used in generating a synthetic data set. Each source has 540 receivers. The recording length is 9 s and the sampling rate is 8 ms. Surface-related multiples can be attenuated by SRME. As an example, shown in Figure 5a is a shot record consisting of primary waves, surface related and internal multiples. Sea bottom and salt boundaries are responsible for most internal multiples, which can be predicted using inverse scattering series. Shown in Figure 5b are extracted internal multiples from the same shot record. A zero-offset profile (Figure 6) is obtained by stacking 1387 internal multiple shot gathers. Applying prestack RTM to shot gathers composed of internal multiples only and using image condition, equations 2 and 3, the UU and DD images are calculated. As discussed in the methodology section, the DD and UU images have similar patterns for real interfaces but different patterns for artifacts. We use this feature and equation 8 to calculate the similarity between DD and UU images to remove unwanted artifacts. The result is shown in Figure 7. The images below salt bodies are correct, but contaminated by specular and non-specular artifacts. There are cross events caused by internal multiples generated inside salt bodies. Three salt bodies are correctly imaged. Because lack of strong deep interfaces to provide upward illumination, the image in the subsalt region is weaker compared to the salt boundaries and can barely be seen.

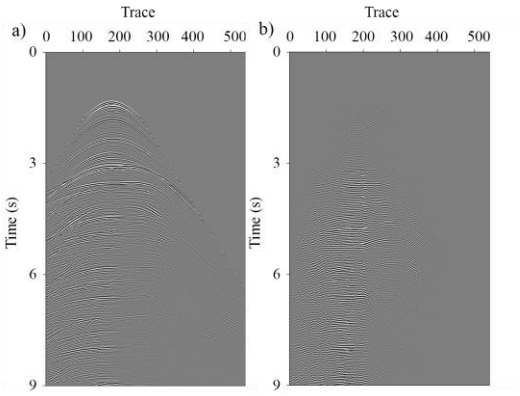

Figure 5. A typical shot gather for SMARRT data set. Left: traces with mixed primary reflections, surface related mulitples and internal multiples. Right: predicted internal multiples, where surface related multiples have been removed.

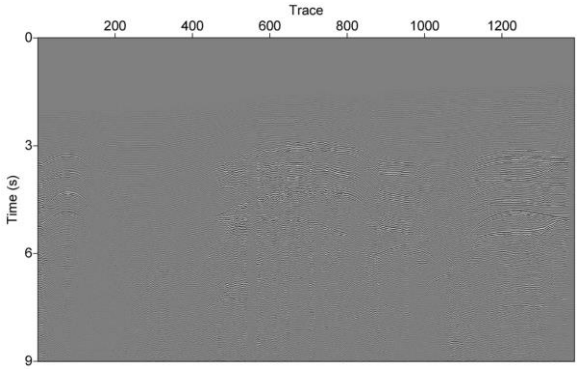

Figure 6. Zero-offset profile by stacking 1387 internal multiple shot gathers

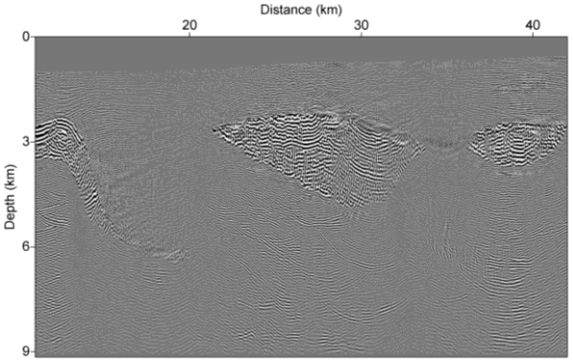

Figure 7. Prestack RTM image from internal multiple only data.

CONCLUSIONS

The new method can properly migrate internal multiples to their correct subsurface locations. In this process, we separate the image into DD and UU parts, where the true image and the artifact behave differently. By comparing their similarities, we can separate artifacts from true images. Correctly predicting various orders of internal multiples, particularly in complicated velocity models, is vital to develop a robust migration algorithm. The SMARRT data set is used to demonstrate the new approach.

ACKNOWLEDGEMENTS

We thank Gerard T. Schuster and Yi Luo for their helpful suggestions and insightful comments. The research was funded by the National Nature Science Foundation of China (Grant No. 41430321, 41374138). We would thank SMAART JV consortium for offering SMARRT data.

DOI http://dx.doi.org/10.1190/segam2015-5760515.1

EDITED REFERENCES

Note: This reference list is a copyedited version of the reference list submitted by the author. Reference lists for the 2015 SEG Technical Program Expanded Abstracts have been copyedited so that references provided with the online metadata for each paper will achieve a high degree of linking to cited sources that appear on the Web.

REFERENCES

Behura, Y., K. Wapenaar, and R. Snieder, 2012, Newton-Marchenko-Rose imaging: 82nd Annual International Meeting, SEG, Expanded Abstracts, doi:10.1190/segam2012-1531.1.

Berkhout, A. J., and D. J. Verschuur, 1997, Estimation of multiple scattering by iterative inversion, Part 1: Theoretical considerations: Geophysics, **62**, 1586–1595, http://dx.doi.org/10.1190/1.1444261.

Broggini, F., and R. Snieder, 2013, Data-driven Green's function retrieval and imaging with multidimensional deconvolution: Numerical examples for reflection data with internal multiples: 83rd Annual International Meeting, SEG, Expanded Abstracts, 4156–4161.

Fleury, C., 2013, Increasing illumination and sensitivity of reverse-time migration with internal multiples: Geophysical Prospecting, **61**, no. 5, 891–906, http://dx.doi.org/10.1111/1365-2478.12041.

Jakubowicz, H., 1998, Wave equation prediction and removal of interbed multiples: 68th Annual International Meeting, SEG, Expanded Abstracts, 1527–1530.

Jiang, Z., J. Sheng, J. Yu, G. T. Schuster, and B. E. Hornby, 2007, Migration methods for imaging different-order multiples: Geophysical Prospecting, **55**, no. 1, 1–19, http://dx.doi.org/10.1111/j.1365-2478.2006.00598.x.

Jin, S., S. Xu, and D. Walraven, 2006, One-return wave equation migration: Imaging of duplex waves: 76th Annual International Meeting, SEG, Expanded Abstracts, 2338–2342.

Liu, F., G. Zhang, S. A. Morton, and J. P. Leveille, 2011, An effective imaging condition for reverse-time migration using wavefield decomposition: Geophysics, **76**, no. 1, S29–S39, http://dx.doi.org/10.1190/1.3533914.

Malcolm, A. E., B. Ursin, and M. V. de Hoop, 2008, Seismic imaging and illumination with internal multiples: Geophysical Journal Internal, **176**, 847–864, doi:10.1111/j.1365-246X.2008.03992.x.

Singh, S., R. Snieder, J. Behura, J. van der Neut, K. Wapenaar, and E. Slob, 2014, Autofocusing imaging: Imaging with primaries, internal multiples and free-surface multiples: 84th Annual International Meeting, SEG, Expanded Abstracts, 4060–4065.

Slob, E., K. Wapenaar, F. Broggini, and R. Snieder, 2014, Seismic reflector imaging using internal multiples with Marchenko-type equations: Geophysics, **79**, no. 2, S63–S76.

Stoughton, D., J. Stefani, and S. Michell, 2001, 2D elastic model for wavefield investigations of subsalt objectives, deep water Gulf of Mexico: 63rd Conference & Exhibition, EAGE, Extended Abstracts, A-33.

Thorbecke, J., J. van der Neut, and K. Wapenaar, 2013, Green's function retrieval with Marchenko equation: A sensitivity analysis: 83rd Annual International Meeting, SEG, Expanded Abstracts, 3888–3893.

van der Neut, J., E. Slob, K. Wapenaar, and J. Thorbecke, 2013, Interferometric redatuming of autofocused primaries and internal multiples: 83rd Annual International Meeting, SEG, Expanded Abstracts, 4589–4594.

Vasconcelos, I., R. Snieder, and B. Hornby, 2007, Target-oriented interferometry — Imaging with internal multiples from subsalt VSP data: 77th Annual International Meeting, SEG, Expanded Abstracts, 3069–3073.

Verschuur, D. J., A. J. Berkhout, and C. P. A. Wapenaar, 1992, Adaptive surface-related multiple elimination: Geophysics, **57**, 1166–1177, http://dx.doi.org/10.1190/1.1443330.

Wapenaar, K., J. Thorbecke, J. van der Neut, F. Broggini, E. Slob, and R. Snieder, 2014, Marchenko imaging: Geophysics, **79**, no. 3, WA39–WA57, http://dx.doi.org/10.1190/geo2013-0302.1.

Weglein, A. B., 2013, The multiple attenuation toolbox: Progress, challenges and open issues: 83rd Annual International Meeting, SEG, Expanded Abstracts, 4493–4499.

Weglein, A. B., F. A. Gasparotto, P. M. Carvalho, and R. H. Stolt, 1997, An inverse-scattering series method for attenuating multiples in seismic reflection data: Geophysics, **62**, 1975–1989, http://dx.doi.org/10.1190/1.1444298.

Zuberi, A., and T. Alkhalifah, 2013, Imaging by forward propagating the data: Theory and application: Geophysical Prospecting, **61**, no. s1, 248–267, http://dx.doi.org/10.1111/1365-2478.12006.